

Possible Nature and Detectability of Endogenic Thermal Anomalies on Europa

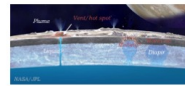
Paul O. Hayne¹, P. R. Christensen², J. R. Spencer³, O. Abramov⁴, C. Howett³, M. T. Mellon⁵, F. Nimmo⁶, S. Piqueux¹, J. A. Rathbun⁴

¹NASA - Jet Propulsion Laboratory, California Institute of Technology (Paul.O.Hayne@jpl.nasa.gov), ²Arizona State University, ³Southwest Research Institute, ⁴Planetary Science Institute, ⁵Applied Physics Laboratory, Johns Hopkins University, ⁶University of California, Santa Cruz

BACKGROUND/MOTIVATION:



How active is Europa at the present time?

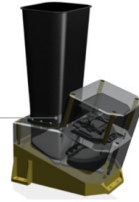


What types of thermal anomalies do models of Europa's ice shell and interior predict?

Previous Work:

Endogenic activity is likely [1] given Europa's young surface age of < 100 Myr [2]. Tidal heating may drive ongoing activity [3, 4]. Temperature is a fundamental indicator of activity [5]. Previous studies have investigated the cooling behavior [6] and detectability [7] of some possible thermal anomalies on Europa, which could be associated with geologic features such as **lenticulae, chaos, ridges and bands**.

The Europa Thermal Emission Imaging System (**E-THEMIS**) is a multi-wavelength infrared instrument designed to search for thermal anomalies as part of NASA's planned Europa Clipper ("multiple flyby") mission. It is based on the highly successful THEMIS investigation at Mars [8].



E-THEMIS rendering (Credit: ASU)

METHODS:

We ran Monte Carlo simulations using a discrete probabilistic model for resurfacing, incorporating temperatures and lifetimes based on numerical thermal models for four feature types: Ridges, Bands, Chaos, Lenticulae.

Likelihood of hot spot occurrence:

- Global average resurfacing rate:

$$\langle \dot{A} \rangle = A/t_{\text{surf}} \sim 1 \text{ km}^2 \text{ yr}^{-1}$$

- Average occurrence rate for feature i with area $A_i (= L_i^2)$ whose total population occupies a fraction of Europa's surface f_i :

$$\langle R_i \rangle = f_i \langle \dot{A} \rangle / A_i$$

- Average time between events i :

$$\bar{t}_i = \langle R_i \rangle^{-1} = \frac{A_i}{f_i \langle \dot{A} \rangle}$$

- Probability of N events during interval Δt , assuming events are independent:

$$P(\Delta t, N) = \left(\frac{\Delta t}{\bar{t}_i} \right)^N \frac{e^{-\Delta t/\bar{t}_i}}{N!}$$

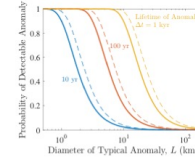


Figure (above): Probability of at least one event occurring during the specified time interval Δt , representing the detectable lifetime for a given thermal anomaly size. Solid lines indicate $\xi = 0.3$; dashed lines indicate $\xi = 0.5$.

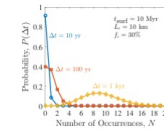


Figure (left): Probability of N events occurring during the specified time interval Δt , representing the detectable lifetime for a given thermal anomaly with dimension 10 km.

Temperatures and lifetimes:

- Buried liquid layer with temperature T_l produces surface anomaly:

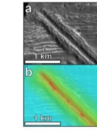
$$\delta T \sim k \frac{T_l - T_s}{4\sigma T_s^3 z}$$

➤ **Maximum detectable depth: ~0.1 – 1 km**

- Shear heating [13] (upper figure): detectable lifetime $\Delta t \sim 10 \text{ kyr}$, $\delta T \sim 5 \text{ K}$

- Freezing and cooling of liquid water ~10 – 100 m thick: detectable lifetime $\Delta t \sim 0.01 – 1 \text{ kyr}$ [6]

- Chaos model: $\Delta t \sim 1 – 10 \text{ kyr}$, $\delta T \sim 163 \text{ K}$ (melting) [6]



Lower figure: melting/warm ice model for a thick layer (> 100 m)

MODEL TIMELINE OF ACTIVITY:

Feature (%):

Feature (%)	A_i	δT_i	Δt
Ridges (50%)	10^4 km^2	5 K	10 kyr
Bands (10%)	10^4 km^2	5 K	10 kyr
Chaos (30%)	100 km^2	163 K	1 kyr
Lenticulae (10%)	100 km^2	162 K	1 kyr
Craters (< 1%)			

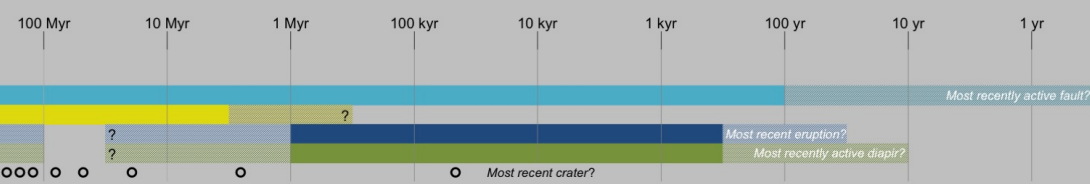
Observations:

Ice Shell, Interior

Geology, Composition

Thermal Properties

Plumes



RESULTS:

Panels at right show example simulation using model parameters above, for a total duration 200 Myr.

The surface temperature "snapshot" is the diurnal mean temperature map at an arbitrary instant in time.

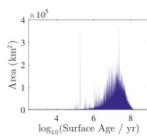
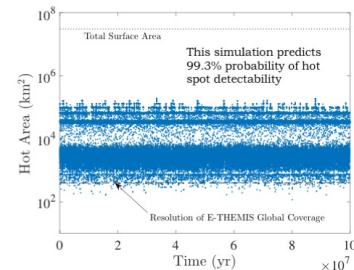
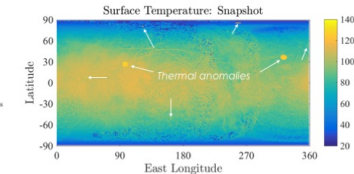
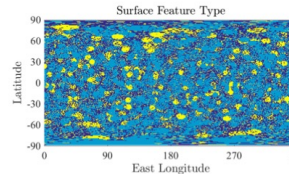
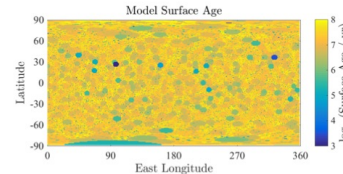


Figure (above): At the end of the simulation, the surface is composed of units of various ages, with an average of ~60 Myr.

Figure (left): Each point represents one instant in time; points above the dashed line are detectable.

Predictions for E-THEMIS:

- Thermal anomalies expected for modeled styles of resurfacing: emplacement of warm ice or liquid water, or shear heating on faults with sufficient dissipation [13]
- Subsurface heat sources (e.g., liquid water) detectable within ~100 m to 1 km
- Daytime and nighttime measurements needed; also visible albedo (right figure)
- Background heat flow could be measured if $>200 \text{ mW m}^{-2}$ at the equator, or $>100 \text{ mW m}^{-2}$ at the pole

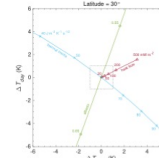


Figure (left): Temperature differences ΔT during the day and night, relative to the background. Error bars indicate uncertainties on individual E-THEMIS measurements. Each point shows expected ΔT values for the given variations in thermal inertia, albedo, and heat flow.

CONCLUSIONS:

Models of Europa's ice shell and interior can be tested by the presence or absence of thermal anomalies:

- Thermal anomalies are likely to be present on Europa today, if resurfacing occurs via warm ice or liquid water, and is either continuous or episodic with recurrence interval < 10 kyr
- Expected thermal anomalies are detectable by E-THEMIS with >99% likelihood for the model above
- Smaller, more frequent thermal anomalies are more likely to be detected, even if they are sub-pixel hot spots

Detection depends critically on accurate measurements of both daytime and nighttime temperature, and visible albedo. NASA's planned Europa Clipper mission and E-THEMIS are being designed to achieve these objectives.

References: [1] Pappalardo, R. T., et al. (1999), *J. Geophys. Res.*, 104E10, 24015-24055. [2] Zahnle, K., et al. (2008), *Icarus*, 194(2), 660-674. [3] Roth, L., et al. (2014), *Science*, 343(6167), 171-174. [4] Sotin, C., et al. (2003), *Geophys. Res. Lett.*, 29(8). [5] Spencer, J. R. (2006), *Science*, 311(5766), 1401-1405. [6] Abramov, O., & Spencer, J. R. (2008), *Icarus*, 193(1), 378-385. [7] Rathbun, J. A., et al. (2010), *Icarus*, 210(2), 763-769. [8] Christensen, P. R., et al. (2004), *Space Sci. Rev.*, 11(1):2, 85-130. [9] Spencer, J. R., et al. (1999), *Science*, 284(5419), 1514-1516. [10] Sredan, J. (1990), *Monatshfte Mat. Phys.*, 1-11. [11] Michael, C., & Manga, M. (2014), *J. Geophys. Res.*, 119(3), 550-573. [12] Manga, M., & Michael, C. (2016), *Icarus*, in press. [13] Nimmo, F., & Gaidos, E. (2002), *J. Geophys. Res.*, 107(14): 14. [14] Siegler, M. A., et al. (2011), *AGU Fall Meeting Abstracts* (Vol. 1, p. 06).

Acknowledgements: This work was supported by the NASA Europa Clipper project. Part of this work was performed at the Jet Propulsion Laboratory, California Institute of Technology, under contract with the National Aeronautics and Space Administration.